Flux cancellation and coronal mass ejections[a)]

Jon A. Linker,[b)] Zoran Mikić, Roberto Lionello, and Pete Riley
Science Applications International Corporation, 10260 Campus Point Drive, San Diego, California 92121

Tahar Amari
Centre de Physique Théorique, École Polytechnique, 91128 Palaiseau Cedex, France

Dusan Odstrcil
University of Colorado, CIRES, and NOAA Space Environment Center, 325 Broadway, Boulder, Colorado 80305

(Received 7 November 2002; accepted 3 February 2003)

Time dependent magnetohydrodynamic computations of the flux cancellation mechanism are presented. Previous authors have discussed this mechanism as a possible cause for the formation of prominences and the trigger for prominence eruptions and coronal mass ejections (CMEs). This paper shows that flux cancellation in an energized two-and-one-half-dimensional helmet streamer configuration first leads to the formation of stable flux rope structures. When a critical threshold of flux reduction is exceeded, the configuration erupts violently. Significant amounts of stored magnetic energy are released through magnetic reconnection. The ejected flux rope propagates out into the solar wind and forms an interplanetary shock wave. A similar eruption occurs for a three-dimensional calculation where the ends of the flux rope field lines are anchored to the Sun. The flux cancellation mechanism unifies the processes of prominence formation, prominence eruption, and CME initiation, and thus provides an attractive hypothesis for explaining the cause of these dynamic events. © *2003 American Institute of Physics.* [DOI: 10.1063/1.1563668]

I. INTRODUCTION

Coronal mass ejections (CMEs) are spectacular, energetic events in the solar corona that expel plasma and magnetic fields into the solar wind. CMEs can create interplanetary shock waves and carry substantial ''southward'' magnetic fields (fields oppositely directed to to the terrestrial magnetic field in the Earth's magnetosphere) and are, therefore, believed to be the primary cause of major geomagnetic storms.[1]

CMEs have been observed since the 1970s.[2–5] They frequently appear as loop-like features that disrupt helmet streamers in the solar corona.[6] Many CMEs exhibit a three part structure, consisting of a bright outer rim, a dark cavity behind the rim, and a bright inner core that is associated with erupted prominence material.[7] Prominences (also referred to as filaments when they are observed against the solar disk), reside above magnetic neutral lines in the photosphere near the base of helmet streamers. They are suspensions of cool ($T\sim10^4$ K), dense ($n\sim10^{10}-10^{11}$ cm^{-3}) chromospheric material in the surrounding hot, tenuous corona ($\sim10^6$ K and 10^7-10^9 cm^{-3}). The prominence magnetic field is observed to be nearly aligned with the filament channel,[8,9] indicating a highly sheared (and therefore, magnetically energized) configuration. Like helmet streamers, prominences can remain stable for days or weeks but at times erupt violently; CMEs and prominence eruptions are closely linked observationally.[10] Figure 1 shows a sequence of images from the Solar and Heliospheric Observatory (SOHO) Large Angle Spectrometric Coronagraph (LASCO) coronagraph[11,12] showing a CME and prominence eruption exhibiting the typical three part structure.

The fundamental theoretical question of how CMEs are initiated has been studied for many years (see reviews by Forbes,[13] Klimchuk,[14] Low[15]), but is still unanswered. It is generally (but not universally, see Chen[16]) believed that the energy that drives CMEs and other forms of solar activity is stored in the coronal magnetic field prior to eruption. Highly nonpotential coronal magnetic fields in active regions have been observed frequently,[17–20] indicating that there is more than enough magnetic energy to drive coronal eruptions. How this energy is released is the key question that must be answered by a successful CME initiation model. Another constraint on CME models is that CMEs open (i.e., drag out into the solar wind) at least a portion of the coronal magnetic field. In strong magnetic field regions low in the corona, the magnetic field pressure dominates both the plasma pressure and the gravitational force, so that fields that are in equilibrium are essentially force-free. Aly[21,22] and Sturrock[23] have shown that $W_{\rm open}$, the energy of the *open field* (for a given magnetic flux distribution, the magnetic field with all field lines beginning at the photosphere and extending to infinity) is the maximum energy for a force-free magnetic field. This appears to present a paradox: how can the magnetic field be opened while releasing energy?

In this paper, we describe how a candidate CME mechanism, ''flux cancellation,'' can fulfill many of the requirements for successfully explaining CME initiation, including dynamic energy release, opening of the magnetic field, and creation of white light signatures similar to observed CME

[a)]Paper BI2 2, Bull. Am. Phys. Soc. **47**, 21 (2002).
[b)]Invited speaker.

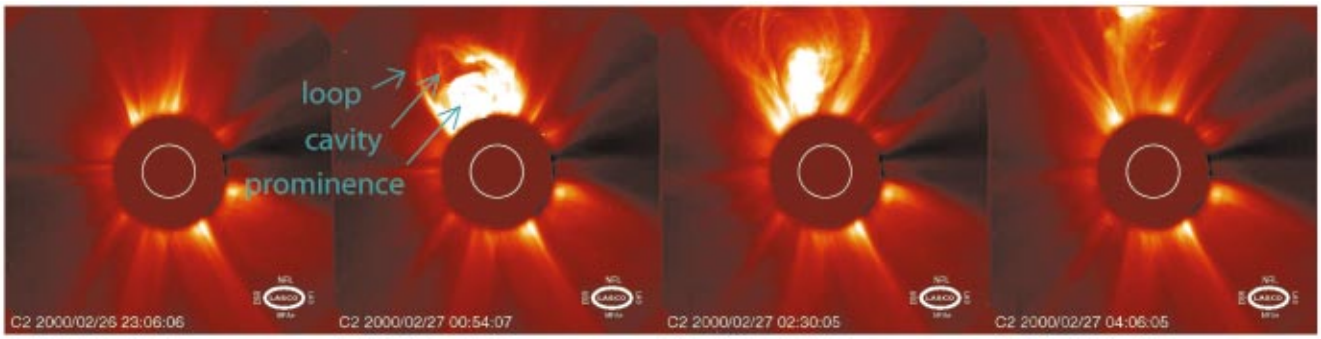

FIG. 1. (Color) A CME observed with the SOHO LASCO C2 Coronagraph, on February 26 and 27, 2000. The dark disk is the occulting disk, and the white circle shows the position of the Sun's surface. The CME shows the typical 3 part structure of a bright loop, cavity, and prominence.

events. In the next section (Sec. II), we describe the mechanism in the context of previous work. Section III briefly describes the methodology of our computations, and Sec. IV shows results for two-dimensional (2D) and 3D computations. Section V summarizes our results.

II. MAGNETIC FLUX CANCELLATION

The magnetic fields in a prominence often exhibit ''inverse polarity,'' meaning that the coronal magnetic fields embedded in the prominence cross over the neutral line in the direction opposite to that indicated by the large-scale photospheric magnetic field polarity. The ingredients for what we refer to here as the ''Flux Cancellation'' mechanism date at least as far back as the Kuperus and Raadu[24] model for inverse polarity promineces. In that model, a current filament (in two dimensions) produces closed magnetic loops that can support prominence material above the photosphere. Since that time there have been a number of authors who have focused on the support of prominence material by helical field lines, and the disruption of these configurations as the possible cause of prominence eruptions and coronal mass ejections.

Flux cancellation has been defined observationally as the mutual disappearance of magnetic fields of opposite polarity at the neutral line separating them.[25] Observations have shown this process to be active at filament sites.[26] van Ballegooijen and Martens,[27] investigating sequences of force-free equilbria, showed that flux cancellation at the neutral line of a sheared arcade configuration leads to the formation of a flux rope. The helical field lines of the flux rope are capable of supporting prominence material, and the rise in the equilibrium height of the flux rope with increased flux submergence suggests possible eruptive behavior. Calculations by Forbes and Isenberg,[28] Forbes, Priest, and Isenberg[29] and Lin *et al.*[30] have show that once a flux rope is formed, continuation of the flux cancellation process can result in a loss of equilibrium. The new lower-energy equilibrium contains a current sheet and a higher height for the flux rope. While the energy release in this ideal process is relatively small, the new equilibrium height of the flux rope can be many solar radii from the Sun. In reality, such an equilibrium is untenable; the flux rope would be pulled outward by the solar wind. Significant magnetic energy release could occur through magnetic reconnection at the current sheet. In this paper, we show that in the context of the resistive MHD equations, flux cancellation does indeed lead to rapid energy release and the disruption of helmet streamer configurations, with material ejected into the solar wind.

III. METHODOLOGY

To compute the consequences of flux cancellation on coronal magnetic fields, we solve the following set of equations in spherical coordinates:

$$\nabla \times \mathbf{B} = \frac{4\pi}{c}\mathbf{J}, \tag{1}$$

$$\frac{1}{c}\frac{\partial \mathbf{B}}{\partial t} = -\nabla \times \mathbf{E}, \tag{2}$$

$$\mathbf{E} + \frac{1}{c}\mathbf{v} \times \mathbf{B} = \eta \mathbf{J}, \tag{3}$$

$$\frac{\partial \rho}{\partial t} + \nabla \cdot (\rho \mathbf{v}) = 0, \tag{4}$$

$$\frac{1}{\gamma - 1}\left(\frac{\partial T}{\partial t} + \mathbf{v} \cdot \nabla T\right) = -T\nabla \cdot \mathbf{v} + S, \tag{5}$$

$$\rho\left(\frac{\partial \mathbf{v}}{\partial t} + \mathbf{v} \cdot \nabla \mathbf{v}\right) = \frac{1}{c}\mathbf{J} \times \mathbf{B} - \nabla p + \rho \mathbf{g} + \nabla \cdot (\upsilon \rho \nabla \mathbf{v}), \tag{6}$$

where $\mathbf{B}$ is the magnetic field; $\mathbf{J}$ is the electric current density; $\mathbf{E}$ is the electric field; ρ, $\mathbf{v}$, p, and T are the plasma mass density, velocity, pressure, and temperature, respectively; $\mathbf{g} = -g_0 \hat{\mathbf{r}} R_s^2 / r^2$ is the gravitational acceleration (with R_s the solar radius); η is the resistivity; and υ is the kinematic viscosity. In the energy equation (5), S includes radiation, thermal conduction, coronal heating, and resistive and viscous diffusion. Lionello, Linker, and Mikic[31] and Linker *et al.*[32] describe calculations that incorporate these processes so as to include the upper chromosphere and transition region in the domain of the calculation. For the goals of this paper (to demonstrate energy release and CME propagation in the co-

rona), it is sufficient to use a ''polytropic'' energy equation, where $S=0$. This approach has the advantage that a relatively simple energy equation can match many of the properties of the corona. However, values of γ close to 1 (1.05 for the results shown here) are necessary to produce radial density and temperature profiles that are similar to coronal observations.[33]

The method of solution of (1)–(6), including the boundary conditions, has been described previously.[32,34–37] The calculation described in Secs. IV A and IV B was performed on on a 201×301 nonuniform (r,θ) grid, with the mesh points highly concentrated near the neutral line and the lower boundary; $\Delta r\approx0.005R_s$ near $R_s=1$ and $\Delta\theta\approx0.24°$ near the neutral line was used.

A uniform resistivity η has been used, corresponding to a resistive diffusion time $\tau_R=4\pi R_s^2/(\eta c^2)=4\times10^4$ hours (for a length scale of R_s). At the base of the helmet streamer, the Alfvén speed (V_{A0}) is about 967 km s^{-1}, the Alfvén travel time ($\tau_A=R_s/V_{A0}$) is 12 min and the Lundquist number $\tau_R/\tau_A\approx2\times10^5$. A uniform viscosity υ is also used, corresponding to a viscous diffusion time $\tau_\upsilon=R_s^2/\upsilon$ such that $\tau_\upsilon/\tau_A=200$.

IV. RESULTS

A. The pre-eruption configuration

CMEs are associated with helmet streamer configurations.[6] To study CME initiation, we first generate a helmet streamer equilibrium (e.g., Linker and Mikić[38]). The procedure is the same as that used for computing the structure of the large-scale corona based on magnetograms.[37,39] We start with a potential magnetic field in the corona that matches a specified distribution of radial magnetic field at the solar surface B_{r0}. Here we choose an azimuthally symmetric B_{r0}, but one that is not symmetric about the equator (the neutral line occurs at $\theta=107°$, 17° below the equator). The magnetic flux distribution is considerably more concentrated than a dipolar distribution; this increases the ratio of the open field energy to the potential field energy (and allows more energy to be stored in an equilibrium configuration). We impose a spherically symmetric solar wind solution and integrate the time-dependent MHD equations in time (for $600\tau_A$, where τ_A is the Alfvén time described in Sec. III) until the solution settles down to an equilibrium. A coronal streamer with closed field lines forms, surrounded by open field lines along which the solar wind flows outward. To investigate the energy release that occurs in CMEs and prominence eruptions, we must introduce free energy into the magnetic field. We apply a shear flow near the neutral line that builds free magnetic energy into the streamer. This shear flow is not intended to model actual flows on the Sun. It is just a convenient mechanism for producing strongly sheared field lines that are nearly aligned with the neutral line, a frequently observed characteristic of filaments.[9] (Present estimates indicate that most of the free energy in active region magnetic fields may actually emerge from below the photosphere when the regions are born, rather than through photospheric flows.[40])

B. Formation of a magnetic flux rope and disruption of the streamer

After the configuration is relaxed in time, a steady-state, energized helmet streamer configuration forms (the energy is about 78% of the corresponding open field energy); The leftmost frames of Fig. 2 ($t=1300\tau_A$) show the pre-eruption configuration. The investigation of the effect of flux cancellation begins at this point in the calculation, when we start to change the magnetic flux at the photospheric boundary. The boundary conditions for evolving the photospheric magnetic flux have been described previously by Refs. 32 and 41. The change in flux is applied by specifying the tangential component of the electric field at the boundary, $\mathbf{E}_{t0}$. For example, when $\mathbf{E}_{t0}=0$, B_{r0} (the radial magnetic field at the solar boundary) remains fixed in time. In order to specify a desired change in the magnetic flux, we specify a nonzero $\mathbf{E}_{t0}$ that is consistent with the required $\partial B_{r0}/\partial t$. This electric field drives converging flows at the neutral line, as is believed to occur in the flux cancellation process.

Flux cancellation (reduction of the flux) first forms a stable flux rope configuration within the helmet streamer (Fig. 2, $t=1350\tau_A$). The high density in the flux rope (seen in the white light image) is reminiscent of a prominence but because of the simplified (polytropic) energy equation, it does not have the correct thermodynamic properties (the plasma is too hot). However, simulations using a more sophisticated energy equation[32] do produce prominence-like (cold) material in the corona. With continued flux cancellation, the helmet streamer is destabilized. At $t=1390\tau_A$ hours the configuration is beginning to move upward rapidly, subsequently erupting into the outer corona ($t=1400\tau_A$), as shown in Fig. 2. Note the formation of a current sheet during the eruptive phase.

Figure 3 shows the time evolution of the magnetic and kinetic energies integrated over the volume of the computational domain for the entire calculation. During the formation of the helmet streamer ($t=0-600\tau_A$), the solar wind opens up the outer field lines of the previously closed potential field and the magnetic energy increases about 15% above the potential magnetic field energy. Energization of the streamer occurs from $t=600-1220\tau_A$, increasing the total magnetic field energy to 3.75×10^{32} ergs. The configuration is then relaxed for $80\tau_A$. The period from $t=0-1300\tau_A$ in the simulation is artificial in the sense it is not intended to model a specific solar process, but to develop an energized helmet streamer configuration suitable for studying the flux cancellation process. Reduction of the magnetic flux commences at $t=1300\tau_A$ and continues to $t=1400\tau_A$, reducing the total magnetic flux by 15%. A detached flux rope first begins to forms at $t=1320\tau_A$ (when the flux is reduced by about 3%), and the eruption begins at about $t=1380\tau_A$ (flux reduction of 12%).

The eruption of the configuration by flux cancellation occurs only when a critical threshold is passed. When flux cancellation is halted with flux reduction levels of 5% and 10%, in both cases the configuration remains stable and

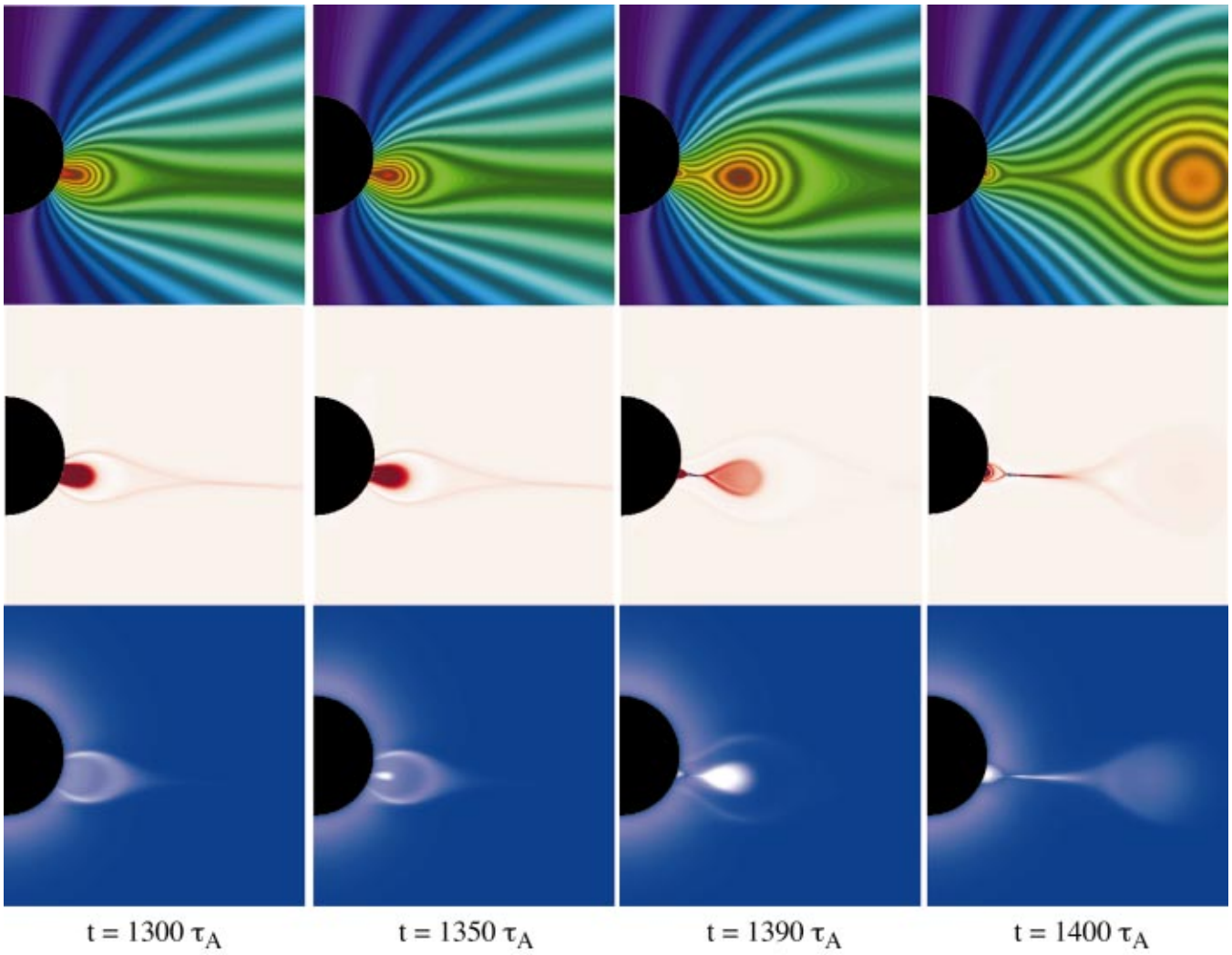

FIG. 2. (Color) MHD Simulation of a helmet streamer eruption triggered by flux cancellation. The stripes in the top panels show projected field lines (there is also a B_ϕ component of the magnetic field out of the plane). The middle panels shows the current density J_ϕ out of the plane. The bottom panels shows the polarization brightness that would be observed by a coronagraph if this were a real CME. A high density flux rope structure can be seen at $t=1350\tau_A$. At $t=1390\tau_A$, the configuration is erupting. This image shows, albeit in an idealized fashion, the 3 part structure observed in many CMEs.

nearly in a steady state; over time the current in the flux rope slowly diffuses because of the finite resistivity in the calculation. Once the configuration is past the eruption threshold, halting the flux cancellation process (e.g., at $t=1380\tau_A$) cannot prevent the eruption. Even for this idealized configuration, a considerable amount of magnetic energy is released during the simulated CME. During the primary energy release phase ($t=1380$ to $t=1420\tau_A$), about 1.75×10^{32} ergs are released, and the kinetic energy increases by 8.7×10^{31} ergs. The remaining energy (not shown) is distributed into heating and gravitational potential energy.

As demonstrated by this calculation and that by Linker *et al.*,[32] prominence formation (i.e., creation of the flux rope) arises as part of the flux cancellation mechanism. Flux cancellation is in turn a natural part of the evolution of the photospheric magnetic field. On the Sun it is frequently observed that the magnetic fields in an active region tend to disperse days to weeks after its emergence. This dispersal of magnetic flux is thought to occur on a small spatial scale by annihilation and submergence of magnetic dipole elements (flux cancellation). During this time, filaments are frequently observed to form along the neutral line, these may erupt at a later time as part of a CME. We have demonstrated that beyond a critical threshold of flux cancellation, our idealized streamer/fluxrope configuration erupts. In the flux cancellation mechanism, the eruption of the filament and the initiation of the coronal mass ejection are different aspects of the same process: The destabilization of the entire magnetic configuration.

The eruption can be viewed from several points of view. First, flux cancellation moves the footpoints of the already sheared magnetic field closer to the neutral line; this reduces poloidal magnetic field (field crossing the neutral line) while the magnetic field tangent to the neutral line is not changed. This has the effect of greatly increasing the shear. Stability of the configuration can also be described as a competition between magnetic pressure forces that tend to expand the configuration and magnetic tension forces that restrain it. Formation and buildup of the flux rope increases the magnetic pressure and removes the stabilizing overlying fields until

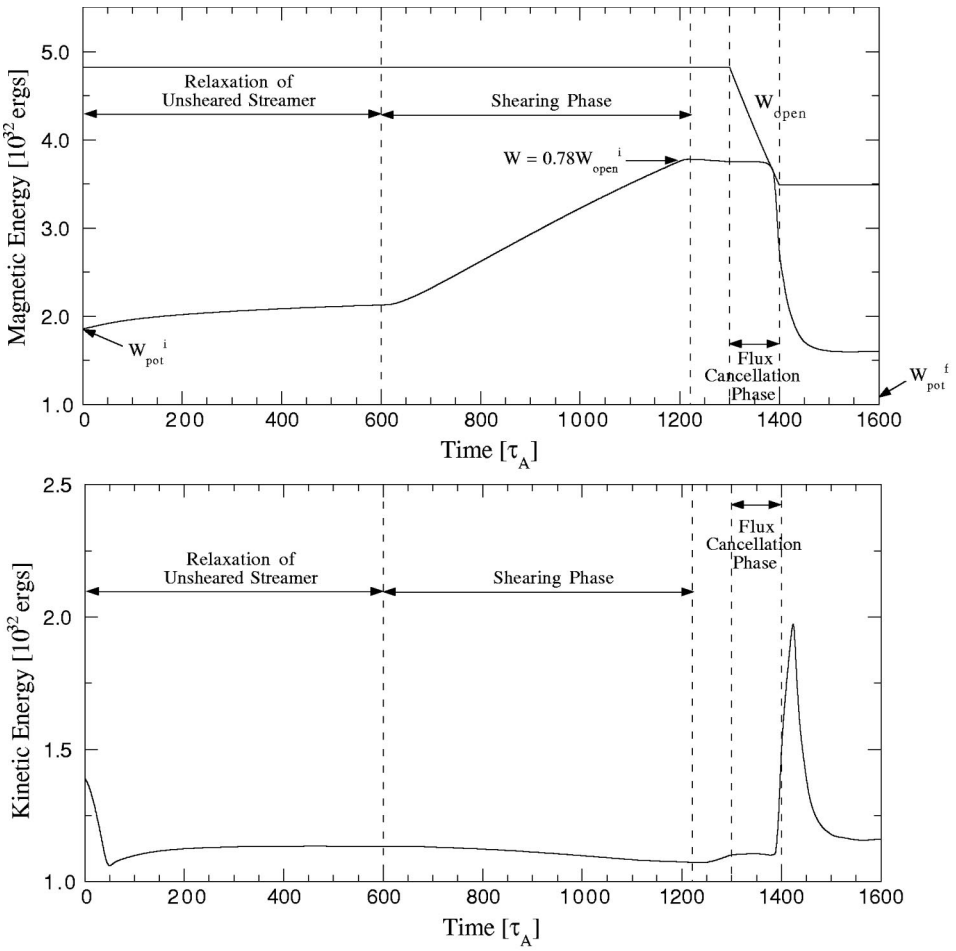

FIG. 3. The magnetic and kinetic energy evolution for the MHD computation shown in Fig. 2. The relaxation and shearing phases of the computation are used to develop an energized helmet streamer configuration, suitable for studying flux cancellation. Flux cancellation begins at $t=1300\tau_A$. The eruption begins at $t\approx 1380\tau_A$, when the open field energy (labeled as W_{open}) approaches the stored magnetic energy in the streamer.

the magnetic field configuration can no longer maintain an equilibrium. It is perhaps most interesting to view the evolution of the system in terms of the energy of the corresponding open magnetic field (W_{open}). The flux cancellation process removes the lowest lying flux near the neutral line, and so significantly affects W_{open}. W_{open} is eventually reduced to the point that the closed field system has a magnetic energy approaching W_{open}, and the configuration erupts. We note that while our solutions are for the full MHD equations (1)–(6) so that our solutions are not in general force-free, W_{open} remains an important parameter for describing the system. This is because the magnetic fields are strongest and most of the magnetic energy is stored near the base of the corona

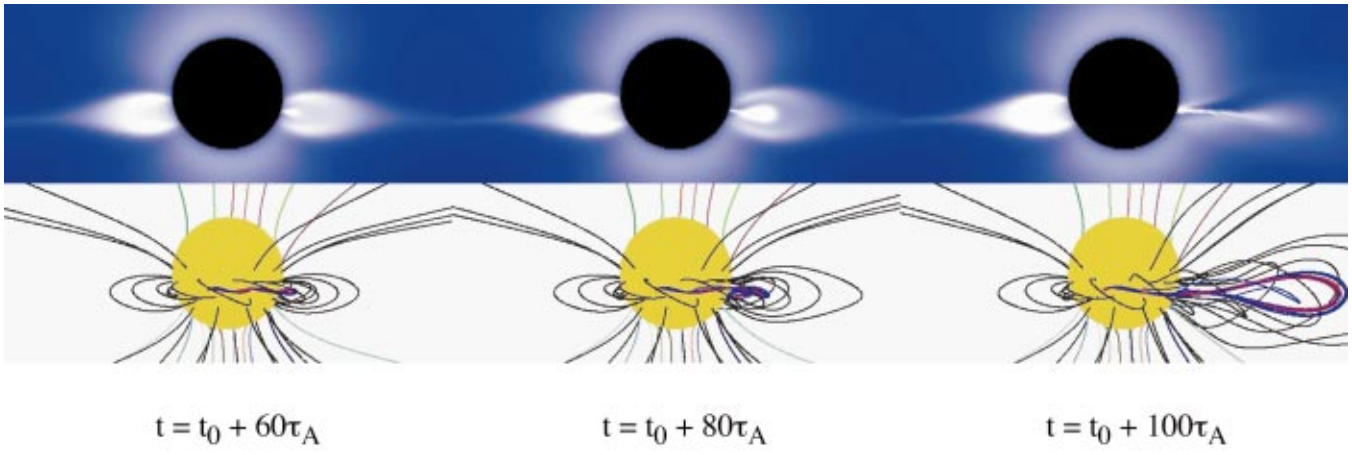

FIG. 4. (Color) Polarization brightness and magnetic field lines for the 3D eruption (see text). The black (yellow) disk in the top (bottom) frames shows the position of the Sun. The viewpoint is slightly above the equator, so the current sheet is not viewed edge on. Black and multi-colored field lines show the helmet streamer and open field lines. At $t=t_0$, flux cancellation begins; flux is canceled only on one hemisphere of the Sun. The blue and red field lines show the flux rope. When a critical threshold for flux cancellation is exceeded, the configuration erupts in a manner similar to the 2D case.

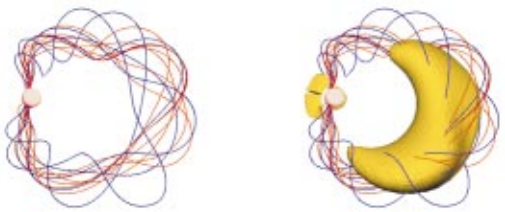

FIG. 5. (Color) Flux rope field lines and an isosurface of the scaled plasma density from the simulation of Fig. 4, looking down from above the north pole of the Sun. The flux rope remains attached to the Sun as it propagates out into the solar wind. The small density surface near the Sun's surface is the unerupted portion of the streamer belt.

where the plasma β is quite low. For magnetic fields to be in equilibrium in this region, they must be very nearly force-free.

C. Flux rope formation and eruption in three dimensions

Azimuthally symmetric models of CMEs suffer from two very unrealistic aspects, the first being that, to some extent, they represent the worst-case scenario for eruption because the entire coronal magnetic field must be opened, not just a portion of it. The second unrealistic aspect is that the flux rope becomes completely detached from the Sun's surface, which is not likely to happen for realistic 3D fields. Amari *et al.*[41] demonstrated a 3D eruption for the flux cancellation process in local Cartesian geometry. Here we show that the streamer disruption we demonstrated in the previous section occurs in 3D as well.

We start from a sheared azimuthally symmetric helmet streamer configuration similar to that discussed in Sec. IV A; the resolution for the 3D calculation was reduced to $81 \times 75 \times 64$ to minimize the computing time. An additional resistivity was added locally based on the current density, to ensure that the current sheet and other dynamically evolving structures were adequately resolved on this coarser mesh. The magnetic flux was now reduced only on one hemisphere of the Sun (centered at longitude 180°) but in the same manner as the 2D case. Figure 4 shows magnetic field lines and the polarization brightness for the 3D eruption. For the 3D case the eruption proceeds similar to the 2D case, but now the ends of the flux rope are anchored in the photosphere. We note that the 3D configuration we have shown here is still very idealized. Flux ropes that would form along real neutral lines are likely to be very complicated.[42] Figure 5 shows an isosurface of the scaled plasma density together with magnetic field lines in the flux rope, after it has propagated away from the Sun.

D. Propagation to 1 A.U.

We do not yet understand how the CMEs observed in the corona evolve to produce the signatures that are measured with interplanetary spacecraft. Clearly modeling must play a key role if we are to clarify this process. Rather than performing a single calculation that encompasses both the inner solar corona and the heliosphere to 1 A.U. and beyond, we have found that it is more efficient to perform the calculation in two separate parts. The first calculation consists of the solution for the inner corona shown above. The second calculation takes the results at the outer boundary of coronal solution as the inner boundary condition for a heliospheric calculation. The MHD characteristics point only outward beyond the sonic and Alfvén points, so backward propagation of information does not occur. Odstrcil *et al.*[43] describe the results of coupling the CME calculation discussed in Secs. IV A and IV B with a heliospheric calculation. In the extended calculation, a flux rope is ejected into the solar wind and a shock wave forms in front of it (Fig. 6). A substantial southward (negative) B_z (relative to the Earth's magnetic field) is also generated. We have also developed a heliospheric solution for the 3D case shown in Sec. IV C, and these results will be discussed in a future paper.

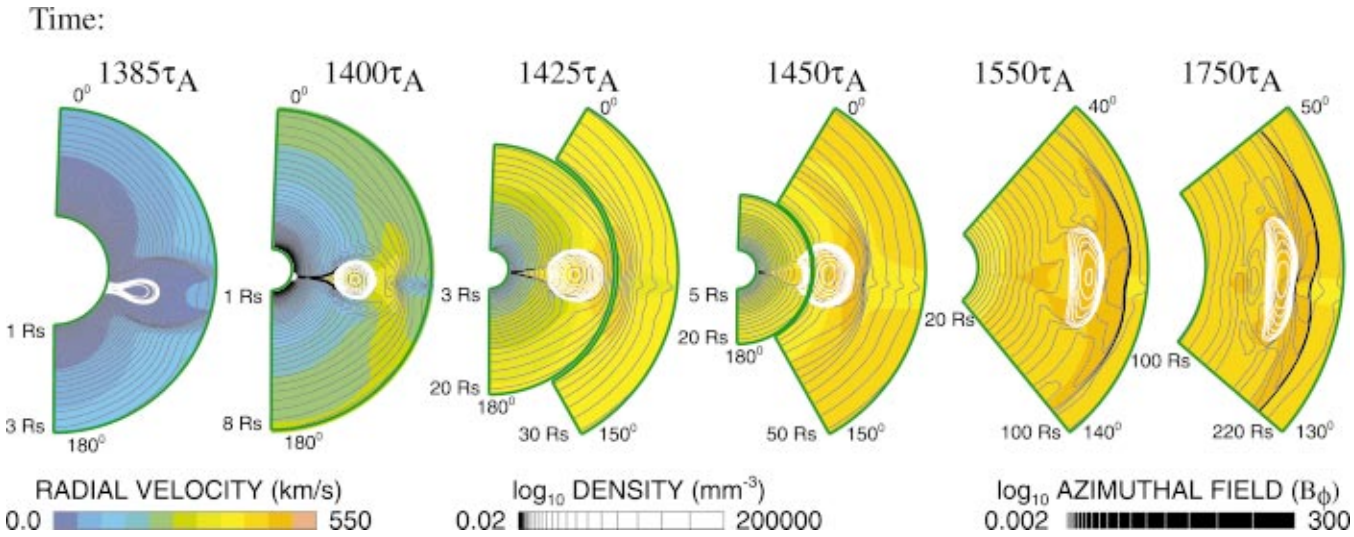

FIG. 6. (Color) The combined coronal and heliospheric calculation of the ejection of the flux rope and formation of a shock wave in the solar wind. The green semi-circle at $20R_s$ marks the boundary between the two calculations. Different portions of the grids are shown in each frame. The white contours of B_ϕ show the position of the flux rope at each time.

V. CONCLUSIONS

The flux cancellation mechanism unifies the processes of prominence formation and prominence eruption with CME initiation, making it an attractive hypothesis for explaining the initiation of CMEs (at least those associated with filament eruptions). We have shown that the mechanism can rapidly release significant amounts of energy and eject plasma and magnetic fields into the solar wind. When the calculation is extended to 1 A.U., an interplanetary shock wave forms.

It is interesting to compare the results of Lin *et al.*[30] with the results shown here. Both calculations are performed in azimuthally symmetric, spherical geometry. While the flux distributions and many other aspects of the calculations are not the same, both calculations show a detached flux rope in equilibrium. It is striking that with a small increase in the flux content of the rope, both calculations show the formation of a current sheet and a dramatic change in the configuration. Lin *et al.*[30] have shown that the change in their configuration is a result of loss of equilibrium. In the time-dependent approach that we employ to obtain our solutions, it is difficult to explicitly identify loss of equilibrium.[34] However, given the similarity of the results, it is plausible that the catastrophe identified by Lin *et al.*[30] is related to the disruption in our simulations. If that is the case, then the magnetic reconnection and rapid energy release observed in our calculations is the consequence of an ideal process.

We note that the flux cancellation process avoids any problems with the Aly–Sturrock energy limit. The ideal process identified by Lin *et al.*[30] does not violate the limit (the fields always remain closed and $W < W_{\text{open}}$; the reconnection that rapidly releases energy in our calculation is a nonideal process not accounted for by the theorem. The flux cancellation mechanism can be contrasted with the idea that prominences emerge as flux ropes from below the photosphere.[15] It is not immediately clear how to distinguish these different processes observationally, as both have similar consequences for flow signatures in the photosphere. If a stable flux rope structure does form in the corona, regardless of the process that formed it, the susceptibility to disruption should not depend on how it originated.

Of course, there are other plausible mechanisms for CME initiation; for example, the ''breakout model.'' [44,45] Why is it so difficult to tell which (if any) of these models is correct? One reason is that the expected observational differences between the models are subtle. For example, distinguishing between field lines that wrap around each other (the ''flux rope'' predicted by flux cancellation) from a collection of strongly sheared dipped field lines (expected from breakout) is quite difficult for realistic fields, particularly when it must be deduced from white-light or emission images. After eruption, the ejected material is embedded in a flux rope in both models, so the CME images that are strongly suggestive of flux ropes unfortunately do not discriminate between these models. Perhaps more importantly, the models have not yet reached the sophistication where, given vector magnetograph data for a specific event, they can be used to predict observable quantities. This is a far more difficult task than generic calculations based on idealized flux distributions, such as we have shown here. This is the challenge that all serious models of CME initiation must confront to ultimately resolve the underlying cause of CMEs.

ACKNOWLEDGMENTS

The images in Fig. 1 are courtesy of the SOHO LASCO instrument. The LASCO data are produced by a consortium of the Naval Research Laboratory (USA), Max-Planck-Institut für Aeronomie (Germany), Laboatoire d'Astronomie (France) and the University of Birmingham (United Kingdom). SOHO is a project of international cooperation between ESA and NASA. This work was supported by NSF Grant Nos. ATM0000950 and ATM0120950 (The Center for Integrated Space Weather Modeling Science and Technology Center), and NASA's SECTP, SR&T, and LWS programs. Computations were performed at the San Diego Supercomputer Center. We also wish to acknowledge beneficial discussions at the SHINE workshops.

[1] J. T. Gosling, J. Geophys. Res. **98**, 18,937 (1993).
[2] R. Tousey, Bull. Am. Astron. Soc. **5**, 419 (1973).
[3] R. M. MacQueen, J. A. Eddy, J. T. Gosling, E. Hildner, R. H. Munro, G. A. Newkirk, Jr., A. I. Poland, and C. L. Ross, Astrophys. J. **187**, L85 (1974).
[4] D. J. Michels, R. A. Howard, M. J. Koomen, and N. R. Sheeley, Jr., *Radio Physics of the Sun*, edited by M. R. Kundu and T. Gergely (Reidel, Hingham, 1980), p. 439.
[5] R. M. MacQueen, A. Csoeke-Poeckh, E. Hildner, L. House, R. Reynolds, A. Stanger, H. Tepoel, and W. Wagner, Sol. Phys. **65**, 91 (1980).
[6] A. J. Hundhausen, J. Geophys. Res. **98**, 13,177 (1993).
[7] R. M. E. Illing and A. J. Hundhausen, J. Geophys. Res. **90**, 275 (1985).
[8] S. F. Martin, R. Bilimoria, and P. W. Tracadas, *Solar Surface Magnetism*, edited by R. J. Rutten and C. J. Schrijver (Kluwer Academic, Dordrecht, 1994), p. 303.
[9] S. F. Martin and C. R. Echols, *Solar Surface Magnetism*, edited by R. J. Rutten and C. J. Schrijver (Kluwer Academic, Dordrecht, 1994), p. 339.
[10] A. J. Hundhausen, *Coronal Mass Ejections*, edited by N. Crooker, J. Joselyn, and J. Feynman (American Geophysical Union, Washington DC, 1997), Geophysical Monograph 99, p. 1.
[11] G. E. Brueckner, R. A. Howard, M. J. Koomen, C. M. Korendyke, D. J. Michels, J. D. Moses, D. G. Socker, K. P. Dere, P. L. Lamy, A. Llebaria, M. V. Bout, R. Schwenn, G. M. Simnett, D. K. Bedford, and C. J. Eyles, Sol. Phys. **162**, 375 (1995).
[12] R. A. Howard *et al.*, *Coronal Mass Ejections*, edited by N. Crooker, J. Joselyn, and J. Feynman (American Geophysical Union, Washington DC, 1997), Geophysical Monograph 99, p. 17.
[13] T. G. Forbes, J. Geophys. Res. **105**, 23,153 (2000).
[14] J. A. Klimchuk, *Space Weather*, edited by P. Song, H. Singer, and G. Siscoe (American Geophysical Union, Washington DC, 2001), Geophysical Monograph 125, p. 143.
[15] B. C. Low, J. Geophys. Res. **106**, 25,141 (2001).
[16] J. Chen, J. Geophys. Res. **101**, 27,499 (1996).
[17] G. A. Gary, R. L. Moore, M. J. Hagyard, and B. M. Haisch, Astrophys. J. **314**, 782 (1987).
[18] M. J. Hagyard, Sol. Phys. **115**, 107 (1988).
[19] R. C. Canfield, J.-F. de La Beaujardiere, Y. Fan, K. D. Leka, A. N. McClymont, T. R. Metcalf, D. L. Mickey, J.-P. Wuelser, and B. W. Lites, Astrophys. J. **411**, 362 (1993).
[20] K. D. Leka, R. C. Canfield, A. N. McClymont, J.-F. de La Beaujardiere, Y. Fan, and F. Tang, Astrophys. J. **411**, 370 (1993).
[21] J. J. Aly, Astrophys. J. **283**, 349 (1984).
[22] J. J. Aly, Astrophys. J. Lett. **375**, L61 (1991).
[23] P. A. Sturrock, Astrophys. J. **380**, 655 (1991).
[24] M. Kuperus and M. A. Raadu, Astron. Astrophys. **31**, 189 (1974).
[25] S. F. Martin, S. H. B. Livi, and J. Wang, Aust. J. Phys. **38**, 929 (1985).
[26] Y. E. Litvinenko and S. F. Martin, Sol. Phys. **190**, 45 (1999).
[27] A. A. van Ballegooijen and P. C. H. Martens, Astrophys. J. **343**, 971 (1989).

[28]T. G. Forbes and P. A. Isenberg, Astrophys. J. **373**, 294 (1991).
[29]T. G. Forbes, E. R. Priest, and P. A. Isenberg, Sol. Phys. **150**, 245 (1994).
[30]J. Lin, T. G. Forbes, P. A. Isenberg, and P. Démoulin, Astrophys. J. **504**, 1006 (1998).
[31]R. Lionello, J. A. Linker, and Z. Mikić, Astrophys. J. **546**, 542 (2001).
[32]J. A. Linker, R. Lionello, Z. Mikić, and T. Amari, J. Geophys. Res. **106**, 25165 (2001).
[33]E. N. Parker, *Interplanetary Dynamical Processes* (Wiley, New York, 1963).
[34]Z. Mikić and J. A. Linker, Astrophys. J. **430**, 898 (1994).
[35]J. A. Linker and Z. Mikić, *Coronal Mass Ejections*, edited by N. Crooker, J. Joselyn, and J. Feynman (American Geophysical Union, Washington DC, 1997), Geophysical Monograph 99, p. 269.
[36]R. Lionello, Z. Mikić, and J. A. Linker, J. Comput. Phys. **152**, 346 (1999).
[37]Z. Mikić, J. A. Linker, D. D. Schnack, R. Lionello, and A. Tarditi, Phys. Plasmas **6**, 2217 (1999).
[38]J. A. Linker and Z. Mikić, Astrophys. J. Lett. **438**, L45 (1995).
[39]J. A. Linker, Z. Mikić, D. A. Biesecker, R. J. Forsyth, S. E. Gibson, A. J. Lazarus, A. Lecinski, P. Riley, A. Szabo, and B. J. Thompson, J. Geophys. Res. **104**, 9809 (1999).
[40]P. Démoulin, C. H. Mandrini, L. van Driel-Gesztelyi, B. J. Thompson, S. Plunkett, Z. Kovári, G. Aulanier, and A. Young, Astron. Astrophys. **382**, 650 (2002).
[41]T. Amari, J. F. Luciani, Z. Mikić, and J. Linker, Astrophys. J. Lett. **529**, L49 (2000).
[42]R. Lionello, Z. Mikić, J. A. Linker, and T. Amari, Astrophys. J. **581**, 718 (2002).
[43]D. Odstrcil, J. A. Linker, R. Lionello, Z. Mikić, P. Riley, V. J. Pizzo, and J. G. Luhmann, J. Geophys. Res. **107**, 10.1029/2002JA009334 (2002).
[44]S. K. Antiochos, Astrophys. J. Lett. **502**, L181 (1998).
[45]S. K. Antiochos, P. J. MacNeice, D. S. Spicer, and J. A. Klimchuk, Astrophys. J. **512**, 985 (1999).